



## Interdiffusion in InGaAs/GaAs: The effect of growth conditions

Khreis, OM; Homewood, KP; Gillin, WP

For additional information about this publication click this link.

<http://qmro.qmul.ac.uk/jspui/handle/123456789/4100>

Information about this research object was correct at the time of download; we occasionally make corrections to records, please therefore check the published record when citing. For more information contact [scholarlycommunications@qmul.ac.uk](mailto:scholarlycommunications@qmul.ac.uk)

# Interdiffusion in InGaAs/GaAs: The effect of growth conditions

O. M. Khreis and K. P. Homewood

*School of Electronic Engineering, Information Technology and Mathematics, University of Surrey, Guildford, Surrey GU2 5XH, United Kingdom*

W. P. Gillin

*Department of Physics, Queen Mary and Westfield College, University of London, London E1 4NS, United Kingdom*

(Received 10 December 1997; accepted for publication 30 March 1998)

The effect of growth temperature and group-V to group-III flux ratio on the intermixing process in molecular beam epitaxially grown  $\text{In}_x\text{Ga}_{1-x}\text{As}/\text{GaAs}$  multiquantum wells were studied by means of photoluminescence coupled with repetitive thermal anneal experiments. We have shown that, for a wide range of growth conditions (growth temperatures from 565 to 636 °C and flux ratios from 5:1 to 25:1) the interdiffusion is controlled solely by a constant background concentration of vacancies which are probably introduced into the substrate during its manufacture. We have shown that, only growth at very low temperatures (470 °C) will result in appreciable excess vacancies. © 1998 American Institute of Physics. [S0021-8979(98)03313-1]

## I. INTRODUCTION

The  $\text{In}_x\text{Ga}_{1-x}\text{As}/\text{GaAs}$  material system is important for optical and electronic devices. Many such devices incorporate quantum wells or heterostructures. Intermixing in III-V heterostructures and quantum wells, particularly in both  $\text{In}_x\text{Ga}_{1-x}\text{As}/\text{GaAs}$  and  $\text{Al}_x\text{Ga}_{1-x}\text{As}/\text{GaAs}$  have been studied for many years under various conditions. These include the anneal ambient, surface encapsulant type, and the effect of ion implantation. Many studies have shown, for example, that samples utilizing  $\text{SiO}_2$  surface encapsulant have higher diffusion coefficients compared with those encapsulated with  $\text{Si}_3\text{N}_4$ .<sup>1,2</sup> In ion implantation, while implanting gallium was found not to affect the intermixing process, implanting arsenic was found to greatly enhance it.<sup>3</sup>

The use of low-temperature grown (450 °C)  $\text{Al}_x\text{Ga}_{1-x}\text{As}$  short period superlattice cladding to improve the performance of InGaAs multiple quantum well (MQW) laser was recently reported.<sup>4</sup> High resistivity low-temperature GaAs (LT-GaAs) buffer<sup>5</sup> and surface<sup>6</sup> layers are becoming increasingly important. The thermal stability of such structures is of interest not just for fundamental studies but also for the possible detrimental effects of intermixing during device processing and the application of intermixing to the developments of new device structures.

The effect of LT-GaAs on the intermixing process in both  $\text{In}_x\text{Ga}_{1-x}\text{As}/\text{GaAs}$  superlattice<sup>7</sup> and  $\text{Al}_x\text{Ga}_{1-x}\text{As}/\text{GaAs}$  quantum wells,<sup>8</sup> have been reported recently. In these studies it was found that the intermixing was enhanced greatly in samples where the top-most layer of GaAs was grown at low temperature when compared with samples where the same layer was grown at normal growth temperature. The enhanced intermixing coefficient was attributed to the high concentration of gallium vacancies in the LT-GaAs layer as a result of excess arsenic. This finding suggests that, the growth temperature, or in general the growth parameters, may affect the intermixing process in semiconductor structures.

This article, presents a study of the effect of growth temperature and group-V to group-III flux ratio on the intermixing process in molecular beam epitaxially grown  $\text{In}_x\text{Ga}_{1-x}\text{As}/\text{GaAs}$  MQWs. For this purpose MQW structures of  $\text{In}_x\text{Ga}_{1-x}\text{As}/\text{GaAs}$  containing seven quantum wells, each of which was grown at different temperature, were grown by molecular beam epitaxy (MBE) using different group-V to group-III flux ratios. Photoluminescence (PL) was used to determine the emission wavelengths of the different quantum wells in the MQW stack. The Schrodinger equation was then solved to determine the compositions of the quantum wells from the PL peaks emission wavelengths. The potential profile in the interdiffused structure was calculated using the error function approach, and the confinement energies were determined by the shooting method.

## II. EXPERIMENTAL DETAILS

The samples used in this work were grown by MBE in a Vacuum Generators V80H reactor on (100) orientated GaAs substrates. The samples consisted of seven quantum wells of  $\text{In}_x\text{Ga}_{1-x}\text{As}$  each of nominal width of 10 nm sandwiched between 50 nm GaAs barriers to provide optical and structural isolation. The growth rate was determined by reflection high energy electron diffraction (RHEED) measurements, and the growth rate for the alloy were kept constant at one monolayer per second. The growth temperature was adjusted during the growth of GaAs barriers, and after some initial test structures, the wells were grown at real temperatures of 470 °C (QW7), 565 °C (QW6), 590 °C (QW5), 610 °C (QW4), 620 °C (QW3), 628 °C (QW2), and 636 °C for QW1, respectively. The initial substrate temperature was determined by reference to the sharp  $C(4\times 4)$  to  $(4\times 2)$  transition in the surface reconstruction monitored by RHEED, at 530 °C for a 5:1 arsenic to gallium flux ratio and subsequently monitored by an optical pyrometer. Details of the growth conditions are given in Ref. 9. Three such wafers were prepared, each of which was grown at a different

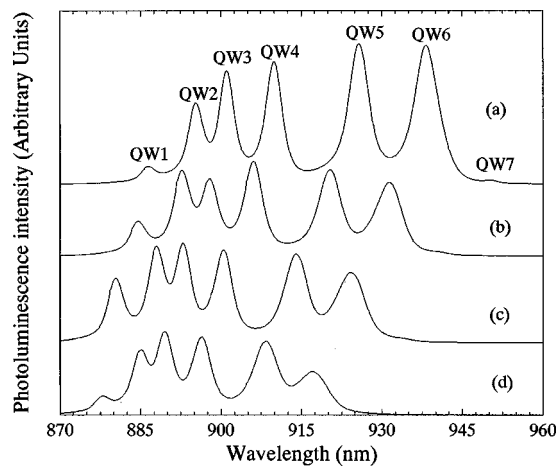


FIG. 1. Photoluminescence spectra of the sample before (a) and after annealing at 950 °C for 15, 30, and 45 s, respectively, (b)–(d).

group-V to group-III flux ratio varied in the range 5:1 to 25:1. The indium composition,  $x$ , of the wells was calculated from the energies of the PL peak positions by solving the Schrodinger equation in the structure to obtain the ground state energies for the conduction and valence band wells, and was found to vary between 0.1 and 0.21. These structures provided a photoluminescence spectra in which all of the quantum well emissions could be easily distinguished (Fig. 1), although the emission from QW7, the well grown at low temperature, is weak as would be expected from the poorer quality material grown at 470 °C.

Following growth the wafers were capped on both the front and back surfaces with 30 nm of silicon nitride. The cap was grown at 300 °C in a plasma enhanced chemical deposition system. The nitride used ( $n=2.1$ ) has been found to give the lowest diffusion coefficient for intermixing in the layers below (i.e., the lowest injection of vacancies), following capping the wafers were cut into 5 mm×5 mm squares for the annealing experiments.

Annealing was performed in a helium ambient using a resistively heated graphite strip heater. The sample was placed between two graphite strips and the temperature measured and controlled using an Accufiber thermometry system. The annealing furnace was calibrated against the melting points of gold, silver, aluminium, and zinc and found to be accurate to 1 °C between 400–1100 °C. Photoluminescence was excited using the 488 nm line of an argon ion laser, and spectra were collected at a sample temperature of 80 K using a liquid nitrogen cooled Ge detector.

In order to measure the diffusion coefficient for intermixing a single sample was repeatedly annealed at a given temperature and the photoluminescence spectra recorded after each anneal. As the quantum well diffuses there is a shift in the peak position to higher energies (Fig. 1). This is caused by the quantum wells effectively narrowing in the early stages of diffusion and subsequently by the reduction in the indium concentration at the well center. By assuming that Fick's law is being obeyed with a constant diffusion coefficient, it is possible to model the shift in the peak position and consequently to calculate the diffusion length for interdiffu-

sion after each anneal. If the square of the diffusion length determined from this analysis is plotted against the anneal time the diffusion coefficient for intermixing can be determined from the gradient of the graph. This procedure is now well established and is presented in more detail by Gillin *et al.*<sup>10</sup>

### III. RESULTS AND DISCUSSION

In Fig. 1 we present typical PL spectra, before and after annealing, for a sample taken from a wafer grown under a typical group-V to group-III flux ratio of 5:1. Figure 1(a) is the PL spectra of the as-grown sample. The seven peaks labeled QW1–QW7 are the  $n=1$  electron to heavy-hole transitions corresponding to the seven quantum wells in the structure. The peak labeled QW1 is the quantum well nearest to the surface grown at 636 °C, while the peak labeled QW7 is the deepest quantum well grown at 470 °C. Figures 1(b)–1(d) are the PL spectra from the same sample after it was annealed at 950 °C for 15, 30, and 45 s, respectively. It can be seen from Fig. 1 that the peak intensity from QW7 is very low for the unannealed sample and rapidly disappears with annealing, which is indicative of the poorer quality growth at 470 °C.

Similar PL spectra to those shown in Fig. 1 were also obtained from the samples taken from the other wafers grown under 20:1 and 25:1 group-V to group-III flux ratios. However, it should be noted that the peak positions of the quantum wells in the different wafers were at different wavelengths. The differences in the PL peak positions of the quantum wells from wafer to wafer are due to indium being desorbed at different rates depending on the flux ratio used during the growth of every wafer and the change of the growth temperature for each well. This resulted in different indium concentrations being incorporated in each well in the different wafers. This process is described in detail in Ref. 9. We have taken this into account and appropriate calibration graphs were constructed accordingly.

The shift in the PL emission wavelengths was monitored as a function of thermal anneal time and temperature. The thermal anneal process leads to a shift in the band gap emission wavelength of the material in the wells through the interdiffusion of the wells and barriers regions and a modification in the electron and heavy-hole sub-band energies from an initial square well potential to a gradually graded potential profile. The shifts in the PL peak positions after annealing were recorded, and by using the method described earlier and in Ref. 10, we can convert the shift for each quantum well into a diffusion length.

Figure 2 shows a graph of diffusion length squared as a function of anneal time for a sample taken from the wafer grown under the typical flux ratio of 5:1. This sample was annealed at 950 °C for times up to 60 s. As  $L_D^2 = 4Dt$ , where  $L_D$  is the diffusion length,  $D$  is the diffusion coefficient, and  $t$  is the anneal time. If the wells were diffusing with a constant diffusion coefficient then we would expect to see the data points for each quantum well lying on a straight line passing through the origin, as we have observed for single quantum wells grown under ideal conditions (see Fig. 4 in

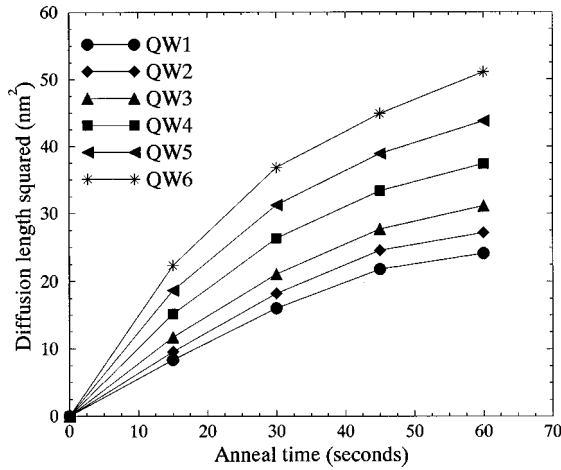


FIG. 2. A graph of the diffusion length squared for all of the quantum wells, calculated from the photoluminescence peak shift, as a function of anneal time, for a sample annealed at 950 °C, and being grown under 5:1 group-V to group-III flux ratio. The lines joining the data points are a guide to the eye.

Ref. 3). However, from Fig. 2, it can be seen that we cannot fit the data points for every quantum well by a simple straight line passing through the origin to determine the interdiffusion coefficient, instead we can see that there are larger gradients at short anneal times which indicates a higher diffusion coefficient. As the annealing progresses these diffusion coefficients reduce to an intrinsic value which is roughly the same for all the quantum wells. It can also be seen from Fig. 2 that the amount of the extra interdiffusion in the wells is a function of the distance of the quantum wells from quantum QW7 (the well grown at 470 °C) with greater interdiffusion being in the well closest to QW7. It should be noted here that the samples taken from the other wafers grown under 20:1 and 25:1 group-V to group-III flux ratios showed similar graphs (not shown here) of anneal time versus diffusion length squared to that shown in Fig. 2. This was also true for all the samples annealed at the temperature range of 800–1000 °C.

It could be argued that as the wells which exhibit the largest initial diffusion coefficients are those with the highest initial indium concentrations then this could be evidence for some effect of indium concentration (i.e., strain) upon diffusion. However, from our earlier work on single quantum wells,<sup>3</sup> where the peak indium concentration is reduced from ~20% to ~10% during diffusion without any change in  $D$ , we do not believe that strain or indium concentration play a role in the diffusivity. In another article we looked at the diffusivity of two samples grown under ideal growth conditions but with varying indium concentrations or well widths.<sup>10</sup> In this work we again found that the initial indium concentration or the well width played no role in determining  $D$ . However, in that work we did find a very small variation in interdiffusion with depth with the diffusion coefficients being slightly greater nearer to the surface, the opposite of that seen in this work. This effect was more than an order of magnitude smaller than the changes seen in this work and was attributed to the small injection of vacancies from the GaAs/SiN<sub>x</sub> interface at the surface.

It is well known that reducing the growth temperature in molecular beam epitaxial growth of InGaAs and AlGaAs layers will result in excess arsenic in these layers.<sup>11</sup> This excess arsenic will produce gallium vacancies which are free to diffuse upon heat treatment. Since the presence of point defects such as vacancies was reported by many workers to enhance the diffusion process in quantum well<sup>8</sup> and superlattice<sup>7</sup> structures, we believe that the extra initial fast diffusion which is seen in all measured samples is the result of the high concentration of gallium vacancies diffusing from the quantum well grown at 470 °C (QW7). In our earlier article<sup>12</sup> we also observed such an effect when we analyzed structures of InGaAs/GaAs similar to those we are investigating in this present article. We will use our earlier vacancy diffusion model<sup>12</sup> to analyze the diffusion process in our present samples.

Initially we assume that QW7 grown at 470 °C is the sole source of excess vacancies. The time evolution of the vacancy diffusion with annealing time can then be expressed as a double error function solution to the diffusion equation, and is given by the following equation:

$$N_{VS}(x,t) = \frac{N_0}{2} \left[ \operatorname{erf} \left( \frac{d/2 - x_0}{2\sqrt{D_V t}} \right) + \operatorname{erf} \left( \frac{d/2 + x_0}{2\sqrt{D_V t}} \right) \right], \quad (1)$$

where  $N_{VS}(x,t)$  is the vacancy concentration due to the source at QW7 as a function of depth and time,  $N_0$  is the initial concentration of vacancies,  $d$  is the thickness of vacancy layer,  $x_0$  is the depth of the layer from the surface,  $t$  is the anneal time, and  $D_V$  is the diffusion coefficient of vacancies. For more details about this vacancy diffusion model see Ref. 12. The model is based on the fact that the diffusion coefficient for intermixing is the product of the concentration of diffusing point defects and their diffusivity,  $D_I = fD_V N_V$ , where  $D_I$  is the interdiffusion coefficient,  $D_V$  is the vacancy diffusion coefficient,  $N_V$  is the concentration of vacancies, which equals the sum of vacancies produced by the low temperature grown quantum well (QW7) plus the background concentration of vacancies in the GaAs material, and  $f$  is the correlation factor which can be taken as being approximately unity. Since the fast diffusion at the early stage of annealing is the result of excess gallium vacancies produced as a result of the low-temperature grown quantum well (QW7), it is possible to calculate the dependence of diffusion length squared as a function of quantum well depth for all the quantum wells in the structure. Using this model it is possible to calculate  $D_V$  and  $N_V$ , where  $N_V$  equals the sum of vacancies from the source at QW7 ( $N_{vs}$ ) plus the background concentration of vacancies in GaAs ( $N_{vb}$ ).

In Fig. 3 we present the depth dependence of the diffusion lengths squared, after the first anneal, for samples taken from the wafer grown under the typical 5:1 group-V to group-III flux ratio. The data points in this figure are the experimentally determined diffusion lengths squared at the first anneal time for three anneal temperatures 800 °C, 850 °C, and 1000 °C plotted as a function of quantum wells depth. The solid lines joining the data points are the theoretical fit using our vacancy diffusion model to solve Eq. (1). The fitting parameters used for these theoretical fits are pre-

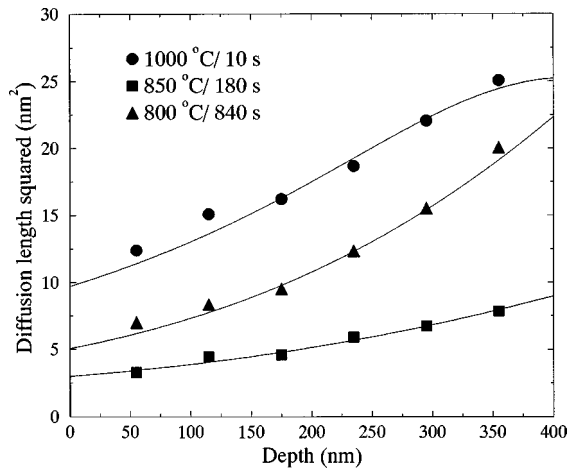


FIG. 3. A graph of the diffusion length squared as a function of depth for samples annealed at 1000, 850, and 800 °C. These samples were grown under the typical 5:1 group-V to group-III flux ratio. The data points are the diffusion length squared for all the quantum wells in the structure calculated at the first anneal time. The solid lines through the data points are the theoretical fit using the values presented in Table I.

presented in Table I. Using these values we can also calculate how the diffusion length for each of the quantum wells should vary as a function of anneal time at any given temperature. Figure 5 shows these theoretical fits at 900 °C along with the experimental data. It can be seen that there is excellent agreement.

Figure 4 shows the experimental diffusion length squared as a function of depth for the samples taken from the wafer grown under a 20:1 flux ratio along with the theoretical fits to the data. Figure 6 shows the time dependence of the diffusion of the wells in this sample, again with the data points being the experimental values and the solid lines being the theoretical fits obtained using the same values as in Fig. 5. Again all the fitting parameters for the 20:1 fit, along

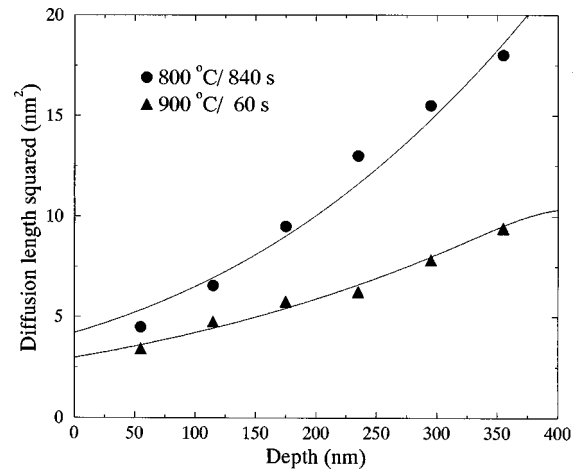


FIG. 4. A graph of the diffusion length squared as a function of depth for samples annealed at 800 °C and 900 °C. These samples were grown under 20:1 group-V to group-III flux ratio. The solid lines through the data points are the theoretical fit using the values presented in Table I.

with those used to fit the 25:1 samples (not shown), are presented in Table I. The most notable thing that can be seen from Table I is that the relative background concentration of vacancies is not a function of the anneal temperature or of the flux ratio during growth but remains constant in all samples at  $\sim 0.5 \times 10^{-5}$ . As the concentration of group-III sites in GaAs is  $\sim 2.2 \times 10^{22} \text{ cm}^{-3}$  this gives a background concentration of group-III vacancies in GaAs of  $\sim 10^{17} \text{ cm}^{-3}$ . This value is in good agreement with our earlier study<sup>12</sup> and references within. We also can calculate from Table I the concentration of excess vacancies produced as a result of the low-temperature (470 °C) grown quantum well (QW7). Remarkably, this concentration also appears to be independent of the V:III flux ratio with a value in all samples of  $\sim 7 \times 10^{19} \text{ cm}^{-3}$ .

These simulations have assumed that, with the exception of the background concentration, QW7 is the only source of vacancies in the structure. While we use 10 nm as the thick-

TABLE I. The vacancy diffusion coefficients,  $D_V$ , relative vacancy concentration in the source at QW7  $N_{VS}$ , and relative background concentration of vacancies in GaAs  $N_{VB}$  used to fit the experimental data points of diffusion length squared vs depth and time. The relative vacancy concentration is the ratio of the number of vacancies to the number of group-III sites.

Flux ratio during growth	Temperature (°C)	$D_V$ ( $10^{-12} \text{ cm}^2/\text{s}$ )	$N_{VS}$ ( $10^{-3}$ )	$N_{VB}$ ( $10^{-5}$ )
5:1	800	0.70	4.20	0.5
	850	1.60	1.25	0.5
	900	14.5	1.00	0.2
	950	50.0	5.00	0.4
	1000	90.0	4.10	0.9
20:1	800	0.70	4.00	0.5
	850	1.60	3.10	0.5
	900	14.5	1.60	0.2
	950	50.0	1.25	0.2
25:1	1000	90.0	7.00	0.9
	800	0.70	4.10	0.4
	850	3.00	1.20	0.7
	900	14.5	3.70	0.6
	950	50.0	3.30	0.5
	1000	90.0	3.10	0.4

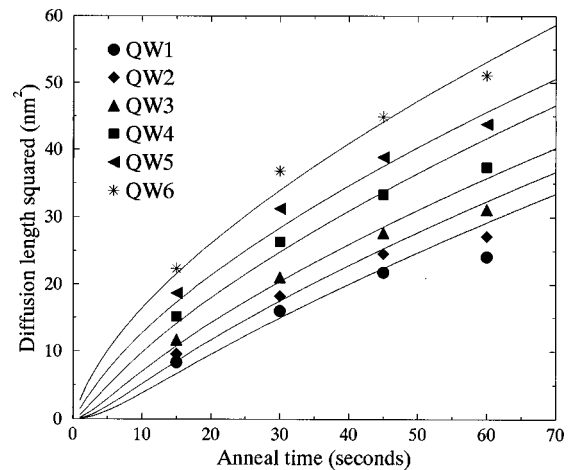


FIG. 5. A graph of diffusion length squared, for the quantum wells, as a function of anneal time, for a sample annealed at 900 °C, for which the group-V to group-III flux ratio was 5:1. The solid lines are the simulations using values presented in Table I.

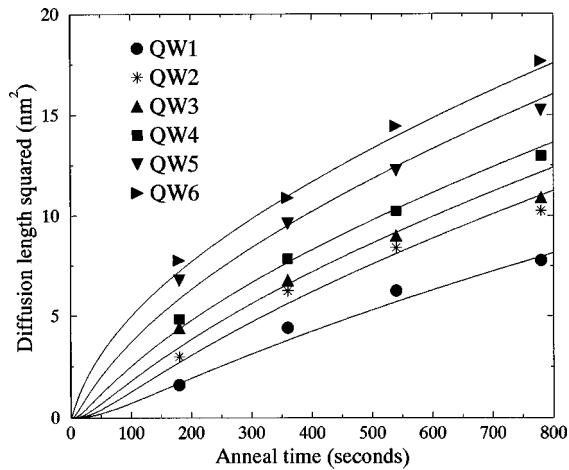


FIG. 6. A graph of diffusion length squared, for the quantum wells, as a function of anneal time, for a sample annealed at 850 °C, for which the group-V to group-III flux ratio was 20:1. The solid lines joining the data points are the simulations using values given in Table I.

ness of the vacancy layer in these simulations, this may not accurately reflect the real distribution of vacancies in the source layer, this is partly because following growth of this layer the substrate temperature was ramped before the next well was grown and consequently there might be some GaAs next to QW7 which is also arsenic rich. However, for the model used to determine the diffusion lengths this will not affect the results, because the diffusion lengths of vacancies are large in comparison to the initial thickness of the source layer, so it is only the thickness concentration product which will affect the concentration of vacancies after annealing. This will however have the effect of increasing the potential error in the calculated initial concentration of vacancies in QW7 (i.e., if the initial vacancy concentration were distributed over 20 nm rather than the 10 nm assumed, the actual vacancy concentrations would be a factor of 2 lower).

Throughout this work we have assumed that only QW7 has any excess vacancies and we have been able to get excellent fits to our experimental results. However, as we have quantum wells which have been grown under such a wide range of growth conditions it would be interesting to determine what concentration of excess vacancies would need to be present in the other wells for them to be seen in these experiments. Obviously the well which would be the most likely to have any excess vacancies after QW7 would be the well which was grown at the second lowest temperature, 565 °C (QW6). In order to determine what concentration of excess vacancies would need to be present in this well for them to measurably affect the diffusion of the structure we modified our simulation to include a source of vacancies at QW6 in addition to those at QW7 and then adjusted the concentration at QW6 until the simulation varied measurably from the experimental results. Using this approach we have shown that if there were a concentration of vacancies in QW6 which was >10% of that in QW7 it would show up in our theoretical model, this concentration is still two orders of magnitude greater than the background concentration. For the other quantum wells the concentration that would be de-

tectable would be lower than this, as the concentration of vacancies which have diffused from QW7 will be lower at any given time the further one is from QW7, in the extreme we could detect excess vacancy concentrations in QW1 which are only slightly above the background value.

These results show that both the growth temperature and the V:III flux ratio for InGaAs/GaAs structure can be varied over quite a large range without seriously affecting the thermal stability of the layers through the introduction of excess vacancies. Rather more interestingly it shows that not only is the background concentration of vacancies which is responsible for diffusion not in thermal equilibrium but that this concentration is independent of both the growth temperature, at least above 565 °C, and of the flux ratio used. This result supports our conclusions in earlier work<sup>12</sup> where we suggested that this background concentration of vacancies is at a value determined by the GaAs substrate and is probably “frozen-in” to the substrate during its growth. This result is in good agreement with an early study of Guido *et al.*,<sup>13</sup> who studied the effect of growth parameters (Fermi-level and group-V to group-III flux ratio) on the intermixing process in  $\text{Al}_x\text{Ga}_{1-x}\text{As}/\text{GaAs}$  and found that the Al–Ga interdiffusion coefficient is independent of the flux ratio.

#### IV. CONCLUSION

We have used a multiple quantum well sample to determine the effect of growth parameters (growth temperature and group-V to group-III flux ratio) on the interdiffusion process of MBE grown InGaAs/GaAs multiquantum well structures. The results show that for a wide range of growth conditions, (growth temperatures from 565 to 636 °C and flux ratios from 5:1 to 25:1) the diffusion is controlled solely by a constant background concentration of vacancies which are probably introduced into the substrate during its manufacture. We have shown that only growth at very low temperatures (470 °C) will result in appreciable excess vacancies.

<sup>1</sup>I. Szafranek, M. Szafrane, J. S. Major, B. T. Cunningham, L. M. Guid, N. Holonyak, and G. E. Stillman, *J. Electron. Mater.* **B20**, 409 (1991).

<sup>2</sup>L. J. Guido, N. Holonyak, K. C. Hsieh, R. W. Kaliski, and W. E. Plano, *J. Appl. Phys.* **61**, 1372 (1987).

<sup>3</sup>I. V. Bradley, W. P. Gillin, K. P. Homewood, and R. P. Webb, *J. Appl. Phys.* **73**, 1686 (1993).

<sup>4</sup>E. C. Larkins, W. Benz, I. Esquivias, W. Rothmund, M. Baeumler, S. Weisser, A. Schronfelder, J. Fleissner, W. Jants, J. Rosenzweig, and J. D. Ralston, *IEEE Photonics Technol. Lett.* **7**, 16 (1995).

<sup>5</sup>F. W. Smith, A. R. Calawa, C.-L. Chen, M. J. Manfra, and L. J. Mahoney, *IEEE Electron Device Lett.* **9**, 77 (1988).

<sup>6</sup>L. W. Yin, Y. Hwang, J. H. Lee, R. M. Kolbas, and R. J. Trew, *IEEE Electron Device Lett.* **11**, 561 (1990).

<sup>7</sup>J. S. Tsang, C. P. Lee, S. H. Lee, K. L. Tsai, and H. R. Chen, *J. Appl. Phys.* **77**, 4302 (1995).

<sup>8</sup>J. S. Tsang, C. P. Lee, S. H. Lee, K. L. Tsai, C. M. Tsai, and J. C. Fan, *J. Appl. Phys.* **79**, 664 (1996).

<sup>9</sup>M. T. Emeny, L. K. Howard, K. P. Homewood, J. D. Lambkin, and C. R. Whitehouse, *J. Cryst. Growth* **113**, 413 (1991).

<sup>10</sup>W. P. Gillin, D. J. Dunstan, K. P. Homewood, L. K. Howard, and B. J. Sealy, *J. Appl. Phys.* **73**, 3782 (1993).

<sup>11</sup>J. F. Whitaker, *Mater. Sci. Eng.*, **B 22**, 61 (1993).

<sup>12</sup>O. M. Khreis, W. P. Gillin, and K. P. Homewood, *Phys. Rev. B* **55**, 15 813 (1997).

<sup>13</sup>L. J. Guido, N. Holonyak, and K. C. Hsieh, *Mater. Res. Soc. Symp. Proc.*, *Inst. Physics Conf. Series* **96**, 353 (1988).